

Published in final edited form as:

ACS Appl Mater Interfaces. 2009 July 29; 1(7): 1504–1511. doi:10.1021/am9001716.

Growth of hydroxyapatite coatings on biodegradable polymer microspheres

Leenaporn Jongpaiboonkit¹, Travelle Franklin-Ford¹, and William L. Murphy^{1,2,3,*}

¹Department of Biomedical Engineering, University of Wisconsin, Madison, WI 53706

²Department of Pharmacology, University of Wisconsin, Madison, WI 53706

³Department of Materials Science and Engineering, University of Wisconsin, Madison, WI 53706

Abstract

Mineral-coated microspheres were prepared via a bioinspired, heterogeneous nucleation process at physiological temperature. Poly(D,L-lactide-co-glycolide) (PLG) microspheres were fabricated via a water-in-oil-in-water emulsion method and were mineral-coated via incubation in a modified simulated body fluid (mSBF). X-ray diffraction, Fourier transform infrared spectroscopy, and scanning electron microscopy with associated energy dispersive X-ray spectroscopy confirmed the presence of a continuous mineral coating on the microspheres. The mineral grown on the PLG microsphere surface has characteristics analogous to bone mineral (termed ‘bone-like’ mineral), with a carbonate-containing hydroxyapatite phase and a porous structure of plate-like crystals at the nanometer scale. Assembly of mineral-coated microspheres into aggregates was observed when microsphere concentrations above 0.50 mg/mL were incubated in mSBF for 7 days, and the size of aggregates was dependent on the microsphere concentration in solution. *In vitro* mineral dissolution studies performed in tris-buffered saline confirmed that the mineral formed was resorbable. A surfactant additive (Tween 20TM) was incorporated into mSBF to gain insight into the mineral growth process, and Tween 20TM not only prevented aggregation, but also significantly inhibited mineral formation and influenced the characteristics of the mineral formed on the surface of PLG microspheres. Taken together, these findings indicate that mineral-coated PLG microspheres or mineral-coated microsphere aggregates can be synthesized in a controllable manner using a bioinspired process. These materials may be useful in a range of applications, including controlled drug delivery and biomolecule purification.

Keywords

mineralization; PLG microsphere; bioinspired; drug delivery; HAP chromatography

I. Introduction

Calcium phosphate-based mineral coatings are desirable interfaces for several biomedical applications, as they are similar in composition to bone tissue, and have been shown to be conducive to the ongrowth and/or ingrowth of newly formed bone. For example, hydroxyapatite - the major inorganic component of bone mineral- has been shown to be osteoconductive,¹ and may also be capable of inducing new bone formation *in vivo*². Another important property of hydroxyapatite is its ability to bind with high affinity to biological

*To whom correspondence should be addressed: William L. Murphy, Department of Biomedical Engineering, University of Wisconsin, 1550 Engineering Drive, Madison, WI 53706, 608-262-2224 (office), 608-265-9239 (fax), wlmurphy@wisc.edu .

molecules. For example, hydroxyapatite has been commonly used as a resin for chromatographic purification of proteins and plasmid DNA^{3,4} because the mineral surface contains both positive (Ca^{2+}) and negative (PO_4^{3-}) ions capable of binding electrostatically with basic and acidic biological molecules, respectively. More recently the high affinity of hydroxyapatite for proteins has also been used as a mechanism to bind and release biologically active molecules, including albumin, BMP-2, TGF- β 1, IGF-1, HGF, and bFGF⁵⁻¹¹. Therefore, a large body of work has focused on creating hydroxyapatite coatings on polymeric biomaterials to exploit the unique advantages of hydroxyapatite coatings.

A particular subset of approaches used to grow hydroxyapatite coatings on biomaterials mimics some aspects of natural biomineralization processes, and has therefore been termed “biomimetic” or “bioinspired”.¹²⁻¹⁶ Kokubo et al. first reported bioinspired growth of apatite coatings on bioactive CaO-SiO₂ glass in a simulated body fluid (SBF), which had ion concentrations nearly equal to those of human blood plasma and was held at physiologic temperature and pH.¹⁷ A series of subsequent studies reported mineral growth using novel formulations of SBF,¹⁸ variation in the mineral growth process,¹⁹ or variations in the base materials.²⁰ The basis for mineral nucleation in these studies involved interactions of mineral ions in solution with polar functional groups on the materials surface, such as Si-OH,²¹ Ti-OH,²² Zr-OH.²³ A series of recent studies has extended the bioinspired mineralization process to include formation of bone-like hydroxyapatite coatings on biodegradable polymer films²⁴ or porous scaffolds.²⁵⁻²⁷ The mechanism for mineral nucleation and growth on these materials is based on the interaction of carboxylate ions and hydroxyl groups on the hydrolyzed surface with calcium- and phosphate-rich nuclei in solution.²⁴ This coating process is particularly suitable for biodegradable polymers, as it can be carried out at physiological temperature and pH,²⁸ and the mild processing conditions have also allowed investigators to co-precipitate minerals with biologically active proteins during the coating process²⁹⁻³³. Therefore, bioinspired growth of mineral coatings may be particularly advantageous in drug delivery applications, enabling protein to be incorporated and released while maintaining biological activity of a released protein^{8,29,34-37}.

In view of the potentially advantageous properties of bioinspired hydroxyapatite coatings, we have developed a bioinspired process to grow hydroxyapatite mineral coatings on the surface of biodegradable polymer microspheres, which are a popular platform in contemporary drug delivery applications. We hypothesized that these microspheres, which have been previously shown to possess a negatively charged surface, would provide a template for bioinspired nucleation and growth of hydroxyapatite. The resulting microspheres are designed to exploit the controllable properties of polymer microspheres (e.g. size, size range, aggregation, degradability, drug incorporation), while also taking advantage of the biological properties of the mineral layer (e.g. biomolecule binding/incorporation). Our processing method had two steps: 1) poly(lactide-co-glycolide) (PLG) microspheres were synthesized using a double emulsion method;³⁸ 2) microspheres were incubated in a modified simulated body fluid, allowing for mineral nucleation and growth in near physiological conditions. A recent communication from our group demonstrated that mineral coatings can be grown on PLG microspheres via this process, and that these coatings can serve as platforms for protein binding and release. The purpose of this more detailed study is to provide a thorough characterization of the mineral growth process and the properties of the resulting mineral layer. In addition, the characteristics of mineral-coated microspheres are modulated in the current study by varying the incubation time, the microsphere concentration, and the presence of surfactant during the coating process. The results presented here illustrate that an inorganic mineral layer can be grown in a controllable manner on the surface of biodegradable microspheres, and these materials may find utility in applications such as drug delivery and protein chromatography.

II. Experimental Section

a. Microsphere fabrication and characterization

85:15 PLG (average $M_w = 50,000$ – $70,000$) and polyvinyl alcohol (PVA, MW 9–10 kDa) were obtained from Sigma-Aldrich (St. Louis, MO). All chemicals and solvents were of reagent grade and were obtained from Fisher Chemicals (Fair Lawn, NJ).

PLG microspheres were fabricated by water-in-oil-in-water (W/O/W) double emulsion technique as report elsewhere^{13,39}. Briefly, the organic phase consisted of 5% (w/v) PLG in 1 ml ethyl acetate. The aqueous phase consisted of 0.1 ml phosphate buffered saline (PBS). The aqueous and organic phases were mixed and sonicated using Sonifier 250 (VWR International, Inc., West Chester, PA) for 15s. The resulting first emulsion was added immediately into 1 ml of aqueous 1% (w/v) PVA in 7% (v/v) ethyl acetate that was being mechanically vortexed for 15 s to form a second emulsion. The resulting solution was then added to a beaker containing 200 ml of 0.3% PVA in 7% ethyl acetate and further rigorously stirred for 4 hr to allow for organic solvent evaporation. The resulting microspheres were collected by filtration through 0.22 μm filter, washed three times with de-ionized water, and resuspended in de-ionized water. The microspheres were lyophilized for a minimum of 48 hr and were stored at -20°C in the presence of a desiccant.

To confirm that PLG microspheres were negatively charged in physiologic buffers, we first characterized the zeta potential of PLG microspheres in PBS and mSBF solutions. The surface charge of the microsphere particles was measured with a Zetasizer (Malvern Instruments 3000HS, UK). Electrophoretic mobility of un-coated microspheres in three, 6mL aliquots was measured to determine the surface potential, with each injection having five measurements. Samples were syringe loaded and measured at 25°C in 1x PBS or mSBF, at a pH of 6.8 to mimic mineral coating conditions.

Quantification of aggregated microspheres in various buffers was performed by incubating 0.5% (w/v) PLG microsphere in selected buffer (1xPBS, mSBF, and mSBF+0.1% Tween 20) for 1, 3, and 7 days. The suspension was held at 37°C and rotated continuously for the duration of the study period, identical to the conditions used for mineral growth. Prior to changing buffer on the subsequent day, aliquots of each condition were taken, diluted 1:8 and imaged under an Olympus Ix51 light microscope at $20\times$ magnification. Four photographs were taken per sample per time point with a Hamamatsu 1394 ORCA-285 camera. The resultant images were viewed and counted using Image J software.

b. Mineral coating of microspheres

PLG microspheres were coated with a mineral layer via incubation in a modified simulated body fluid (mSBF) for 7 days. The mSBF solution was replaced daily to ensure adequate ion concentrations for mineral growth. mSBF possesses inorganic ion concentrations similar to those of human blood plasma, with 2X the concentration of calcium and phosphate ions. mSBF was prepared by dissolving 141 mM NaCl, 4.0 mM KCl, 0.5 mM MgSO_4 , 1.0 mM MgCl_2 , 4.2 mM NaHCO_3 , 5.0 mM CaCl_2 , and 2.0 mM KH_2PO_4 in distilled water, buffered to pH 6.8, and was held at 37°C for the duration of the incubation period. In some experiments, 0.1% of Tween 20TM (Sigma-Aldrich, St. Louis, MO) was added to the mSBF to influence the aggregation of microspheres.

c. Materials characterization

The composition and phase of the minerals grown on polymer microspheres were analyzed using a HI-STAR 2D x-ray diffractometer (Siemen Corporation, NY) operating at 40kV and 20 mA. X-ray diffraction spectra were taken for $2\theta = 20$ – 40° and data collection was controlled

using General Area Detector Diffraction System (GADDS) version 4.0 (Bruker AXS Inc., Madison, WI).

Fourier transform infrared spectroscopy (FTIR) data were obtained using EQUINOX 55 spectrometer (Bruker AXS Inc., Madison, WI). Samples were examined in transmission mode in the 400 – 4000 cm^{-1} range and data were analyzed by OPUS software.

The morphology and composition of the coated mineral on the microsphere surface was analyzed using scanning electron microscopy (SEM) with energy-dispersive X-ray spectroscopy (EDS). Microspheres before and after mSBF incubation were mounted on aluminum stubs with double sided carbon tape, sputtered with gold for 30s at 45mA and characterized using a LEO DSM 1530 field emission SEM, operating at 2kV for SEM and 10kV for EDS.

Dissolution of mineral coatings was characterized by measuring release of PO_4^{3-} and Ca^{2+} over 25 days in multiple solutions, including tris-buffered saline (150mM NaCl and 20mM Tris, pH = 7.4) or Dulbecco's Modified Eagle Medium (DMEM) without L-glutamine and phenol red (Mediatech, Inc., Manassas, VA). 5mg of mineral-coated microspheres were immersed in 1ml buffer solution and incubated with continuous rotation for 24h at 37°C. The buffer was collected and refreshed daily. The study was performed in triplicate and held at 37°C for the duration of dissolution study period.

The amount of phosphate released from mineral-coated microspheres was analyzed colorimetrically using an assay previously reported.⁴⁰ Briefly, a working AAM (acetone-acid-molybdate) solution was prepared by mixing 2 parts acetone with 1 part 5N sulfuric acid, and 1 part 10mM ammonium molybdate solution. The assay was performed in a 96-well plate by adding 100 μl a freshly made working solution to 100 μl sample. The amount of phosphate complex was quantitatively detected by measuring the absorbance at 405 nm on a Synergy™ HT Multidetector Microplate Readers (Bio-Tek Instruments, Inc., UK) and comparing to a set of standards with known phosphate concentrations.

Ca^{2+} release was direct measured using QuantiChrom™ Calcium Assay Kit (DICA-500) (BioAssay Systems, Hayward, CA). A phenolsulphonophthalein dye forms a very stable blue color complex with free calcium. The intensity of the complex, measured via absorbance at 612nm, was used to measure released Ca^{2+} by comparing to a set of standards with known calcium concentrations. Dissolution experiments were performed in triplicate and the average of calcium and phosphate release were reported.

III. Results and Discussion

Fabrication and characterization of PLG microspheres

A double emulsion process detailed in previous studies^{38,39} was used here to produce spherical particles of 85:15 PLG (Fig. 1A). The zeta potential of these particles in PBS (-81.09 ± 7.71 mV) and mSBF (-78.62 ± 15.91 mV) indicated that the particles were negatively charged (Fig. 2A). These zeta potential values are consistent with previous studies of PLG microspheres, which have also shown that PLG microspheres have negatively charged surface carboxylate groups,⁴¹ and that they have zeta potential values ranging from -22 to -80 , depending on the microsphere preparation technique and the testing buffer.^{42–45} The presence of carboxylate groups on the surface of these microspheres is important, as previous studies have indicated that these groups are capable of promoting heterogeneous mineral nucleation and growth. However, in previous studies PLG materials were hydrolyzed to produce surfaces containing carboxylate ions, while in this case the PLG microsphere surfaces included negatively charged groups when synthesized via double emulsion processing without additional hydrolysis.

Interestingly, the zeta potential of PLG microspheres was significantly lower than hydrolyzed PLG films used previously as templates for bioinspired mineral nucleation and growth (Fig. 2B),²⁴ suggesting that the microspheres may serve as advantageous templates for mineral growth.

Mineral nucleation and growth

Incubation of PLG microspheres in mSBF led to nucleation and growth of a hydroxyapatite mineral coating on the microsphere surface (Fig. 1B). SEM observation showed that the nanocrystallites grown on the microsphere surface exhibit a plate-like morphology (Fig. 3), similar to the morphology observed in native bone tissue and in previous bioinspired mineral growth studies^{31,46}. Micrographs of the microspheres incubated in mSBF for 7 days show continuous mineral coatings on individual microspheres incubated at 0.25% and 0.50% (w/v) (Fig. 3A, B). Microsphere aggregation was observed as microsphere concentration increased, and mineral coatings were also observed on the surface of microsphere aggregates (Fig. 3C, D). Zeta potential results showed charged microspheres in all buffers tested (Fig. 2A), so it is possible that the presence of salt leads to shielding of microsphere surface charge, thereby limiting electrostatic repulsion and facilitating aggregation. The size of the aggregates increases with microsphere concentration, as the size of microsphere aggregates was proportional to the initial microsphere concentration in solution (Fig. 3E). To determine whether the aggregation of the microspheres was due to some intrinsic property of mSBF, we performed aggregation experiments in which microspheres were incubated in three different solutions: 1) a 1X phosphate buffered saline solution (calcium deficient), 2) mSBF, and 3) mSBF in the presence of Tween20. Each incubation was performed at 37 degrees C with daily solution changes for 7 days. Results showed 35% and 42% of microspheres aggregated after the first day of incubation in PBS and mSBF, respectively. The percentage of aggregated microspheres increased to 87% in PBS and 90% in mSBF after 7 days of incubation. In contrast, the number of microspheres aggregated in mSBF supplemented with Tween20TM was significantly lower at each time point (Supp. Fig. 1). These data indicate that mSBF does not significantly increase microsphere aggregation when compared to PBS, and the presence of Tween20TM significantly decreases microsphere aggregation.

Characteristics of mineral coatings

The phase and composition of mineral coatings on PLG microspheres after a 7 day incubation in mSBF were characterized by XRD and FTIR. XRD spectra of mineral-coated microspheres show three characteristic hydroxyapatite peaks at $2\theta = 25.87^\circ$, 28.68° , and 32.05° similar to the peaks present in the XRD spectrum of reagent grade hydroxyapatite powder (Sigma-Aldrich, St. Louis, MO) at $2\theta = 26^\circ$, 28.5° , and 32° (Fig. 4A). The peak areas in the XRD spectrum of mineral-coated microspheres are broader than that of hydroxyapatite powder, and this may be due to the small crystal size of the mineral deposited on the PLG microsphere surfaces. FTIR peaks observed in the $1600\text{--}400\text{ cm}^{-1}$ region can be attributed to carbonate-substituted hydroxyapatite, including phosphate peaks at 570 , 950 , 1046 , and 1098 cm^{-1} , and carbonate peaks at 870 , 1410 , and 1456 cm^{-1} . The EDS spectrum also confirms the presence of Ca and P on the mineral-coated microspheres (Fig. 4C). The Ca/P ratio of the mineral coating was 1.41 after 7 days incubation in mSBF, which is consistent with previous studies of biological apatites⁴⁷ and bioinspired mineral coatings.⁴⁶

Time-lapse SEM analyses of PLG microspheres during mSBF incubation provide some insight into the mechanism of nucleation and growth of carbonate apatite mineral on aggregating microspheres (Fig. 5). The nucleation process begins during the first three days of incubation in mSBF (Fig. 5A, B). During this stage the aggregation of microsphere begins to occur. As the microspheres begin to aggregate, small crystals ($\sim 2\text{--}10\text{ nm}$) begin to form at the interface between microspheres (Fig. 5A, B), perhaps due in part to local supersaturation of functional

groups at adjacent microsphere interfaces, and associated mineral ions at the interfaces. Our data also suggest that aggregation is not a pre-requisite for mineral nucleation and growth, as at low concentrations of microspheres in solution (0.25–0.50% w/v) we observed individual microspheres coated with mineral (Fig. 3A, B). However, aggregation could have a positive impact on mineralization, and the processes could occur simultaneously. After five days a porous structure of plate-like hydroxyapatite crystals appear on the surfaces of aggregated microspheres (Fig. 5C), ultimately growing into a continuous coating (Fig. 5D). The size of the aggregates depends on the initial concentration of microspheres in solution (Fig. 3E), and mineral coatings were also observed on the surface of microsphere aggregates. Other analyses not presented here suggest that the efficiency of microsphere mineralization increases in conditions that promote microsphere aggregation. Our time-course analysis of mineral formation in solutions with higher concentrations of microspheres (Fig. 5) also demonstrate that mineral nucleation can occur at the interface between aggregated microspheres (e.g. Fig. 5B), which suggests that mineral formation can be facilitated by aggregation.

Interestingly, the mineral described here is analogous to previous bioinspired mineral formation by He et al.⁴⁸, in which mineral was formed in the presence of dentin matrix protein. In addition, the morphology and composition of mineral described here is similar to the apatite found in human bone and mineralized dentin,⁴⁹ specifically a plate-like nanostructure (Fig. 1B and 8B), hydroxyapatite phase (Fig. 4A, C), and carbonate-substitution (Fig. 4B).

Dissolution is a key characteristic of hydroxyapatite coatings, particularly in potential drug delivery applications in which drug release has been shown to be dependent on mineral dissolution rate. Therefore, in this study we characterized dissolution of mineral coatings in tris-buffered saline (TBS) and in DMEM for 25 days. Ca^{2+} and PO_4^{3-} were gradually released from mineral coatings over time in TBS (Fig. 6A), indicating that these coatings are less stable than pure, stoichiometric hydroxyapatite characterized in previous studies.^{13,50,51} The total amounts of Ca^{2+} and PO_4^{3-} released after 25 days in TBS were 15.87 and 10.26 μMol , respectively, and the dissolution data indicated a Ca/P mol ratio in the range of 1.37–1.61 during the course of the 25 day study, indicating that the stoichiometry of the dissolving mineral may vary during the time course of dissolution. SEM images obtained at the end of the dissolution study also demonstrate a significant level of resorption of the mineral coating in TBS (Fig. 6B) when compared to the initially coated microspheres (Fig. 5D). The increased dissolution rate of these coatings when compared to pure hydroxyapatite coatings used in clinical applications can be explained by differences in crystallinity and carbonate substitution in the mineral. Fazan and Marquis⁵⁰ reported previously that the dissolution rate of plasma-sprayed hydroxyapatite coatings decreases with an increase the degree of crystallinity of the hydroxyapatite. In addition, it has been reported that incorporation of sodium and carbonate ions into calcium phosphate minerals, such as hydroxyapatite, dramatically increases the dissolution rate,⁵² and our FTIR analyses clearly indicate the presence of carbonate ions in the mineral coatings (Fig. 4B).

When mineral-coated microspheres were incubated in serum-free DMEM, there was a decrease in the cumulative amount of $(\text{PO}_4)^{3-}$ in the dissolution media over time (Fig. 6C), indicating that phosphate-containing mineral could possibly be re-precipitating on the surface of the mineral coating due to the ion exchange between the carbonate-substitute hydroxyapatite and the $(\text{PO}_4)^{3-}$ in DMEM. This result suggests that the mineral coating could possibly serve as a substrate for nucleation of a calcium phosphate mineral component in the DMEM solution (Fig. 6D). SEM images indicated that the morphology of the mineral coating after incubation in DMEM was similar to the morphology of the mineral prior to incubation in DMEM, which suggests that if re-precipitation is occurring, it is resulting in growth of a new mineral phase that is similar to the mineral phase grown initially. These results are consistent with previous work, in which hydroxyapatite was immersed in either TBS or a modified Hank's-buffered

saline (HBS) solution, which had an ionic composition similar to human plasma.⁵¹ In tris buffer there was no new mineral formed on the hydroxyapatite surface, while in the modified HBS solution an apatite coating was grown on the surface, and this new mineral coating had a similar morphology to the initial hydroxyapatite surface.

Previous studies have shown that drug release kinetics from the surface of hydroxyapatite are comparable to the hydroxyapatite mineral dissolution kinetics.^{13,53} Therefore, the aggregation of the mineral-coated microspheres is likely to slow drug release due to the reduction in the surface area. Multiple recent studies have shown that protein release kinetics from the surface of hydroxyapatite strongly depends on the pH of the buffer medium.^{13,54} For example, Matsumoto et al. demonstrated that enhanced mineral dissolution at low pH can lead to increased protein release. Based on these previous studies, we hypothesized that composition and pH of buffer media would have an impact on dissolution rate of the mineral. This hypothesis is supported by our data indicating that mineral dissolution rate is highly impacted when incubating mineral-coated microspheres in either tris-buffered saline (TBS) and in DMEM (Fig. 6A, B). Ions were gradually released from the mineral over time in TBS (Fig. 6C), whereas re-precipitation of mineral occurred in phosphate-containing media (Fig. 6D). This newly deposited mineral could interfere with drug diffusion out of the initially coated mineral, thereby slowing drug release.

Effect of surfactant on mineral nucleation and growth

In order to modulate aggregation of microspheres and observe effects on mineral growth, Tween20™ was added to the mSBF solution. Tween20™ is a common surfactant used as a stabilizer in studies which measure drug release from PLG microspheres *in vitro*.^{55,56} Mineral formation on the surface of microspheres is inhibited in the presence of Tween20™ (Fig. 7A–D) when compared to mineral formation in the absence of surfactant (Fig. 1, 3). FTIR spectra of the mineral formed in the presence of surfactant (Fig. 7E) show peaks in the range of 650–800 and 1108–1414 cm^{-1} , which indicate the presence of PO_4^{3-} similar to the mineral formed in the absence of surfactant (Fig. 4B) and to synthetic HA (Fig. 7E). The FTIR spectrum also included CO_3^{2-} peaks at 1410, and 1450 cm^{-1} which were absent in synthetic HA (Fig. 7E). SEM images of the mineral formed in the presence of Tween20™ show scattered islands of nanometer-scale mineral formation. Interestingly, the morphology of the mineral coatings in the presence of surfactant also differs significantly from the nanometer-scale plate-like morphology apparent in the coatings formed without surfactant (Fig. 8A–B). This result suggests that surfactant addition could be used in future studies as a mechanism to vary mineral morphology on the microsphere surface, which could have implications for mineral degradation, binding of biological molecules, and biological activity. For example, a rough surface with a relatively well-distributed mineral coating has an increased surface area, and the corresponding increase in available binding sites could result in higher protein binding.^{13,57}

IV. Conclusion

Mineral-coated PLG microspheres have been fabricated via a bioinspired process, which can be varied to modulate the resulting microsphere properties. XRD and FTIR spectra indicated that the coatings comprised a carbonated-substituted hydroxyapatite mineral with a porous, plate-like microscale morphology. The size of the mineral-coated microspheres or mineral-coated microsphere aggregates can be controlled by varying the microsphere concentration in the mSBF solution. Hydroxyapatite coatings were degradable in tris-buffered saline, and analysis of calcium and phosphate release from the coatings indicated that the Ca/P molar ratio in the mineral is consistent with that of carbonated-substituted hydroxyapatite. The presence of a surfactant during the mineral growth process partially inhibited the formation of mineral,

and also significantly affected the morphology of the mineral. Taken together, these findings indicate that mineral-coated PLG microspheres can be synthesized in a controllable fashion using a bioinspired process. This material may be useful in a variety of applications that may benefit from the bulk properties of polymer microspheres and the surface properties of hydroxyapatite minerals, including drug delivery and biomolecule purification.

Supplementary Material

Refer to Web version on PubMed Central for supplementary material.

Acknowledgments

This work was supported by the Wallace H. Coulter Foundation (Translational Research Partnership Grant) and the National Institutes of Health (R03AR052893). The authors also thank to Claire Edlebeck for collecting data for the mineral dissolution study.

References

1. Ducheyne P, Qui Q-Q. *Biomaterials* 1999;20:2287–2303. [PubMed: 10614935]
2. Habibovic P, Sees TM, van den Doel MA, van Blitterswijk CA, de Groot K. *J. Biomed. Mater. Res., Part A* 2006;77A:747–762.
3. Colman A, Byers MJ, Primrose SB, Lyons A. *Eur. J. Biochem* 1978;91:303–310. [PubMed: 363426]
4. Schroder E, Jonsson T, Poole L. *Anal. Biochem* 2003;313:176–178. [PubMed: 12576076]
5. Alt V, Pfefferle HJ, Kreuter J, Stahl JP, Pavlidis T, Meyer C, Mockwitz J, Wenisch S, Schnettler R. *J. Control Release* 2004;99:103–111. [PubMed: 15342184]
6. Blom EJ, Klein-Nulend J, Wolke JG, van Waas MA, Driessens FC, Burger EH. *J. Biomed. Mater. Res* 2002;59:265–272. [PubMed: 11745562]
7. Hossain M, Irwin R, Baumann MJ, McCabe LR. *Biomaterials* 2005;26:2595–2602. [PubMed: 15585262]
8. Liu Y, Hunziker EB, Layrolle P, De Bruijn JD, De Groot K. *Tissue Eng* 2004;10:101–108. [PubMed: 15009935]
9. Ripamonti U, Yeates L, van den Heever B. *Biochem. Biophys. Res. Commun* 1993;193:509–517. [PubMed: 8390243]
10. Sumner DR, Turner TM, Urban RM, Viridi AS, Inoue N. *J. Bone. Joint Surg. Am* 2006;88:806–817. [PubMed: 16595471]
11. Zamboni G, Grano M, Greco G, Oreffo RO, Triffitt JT. *Acta. Orthop. Scand* 1999;70:217–220. [PubMed: 10366928]
12. Hong L, Wang YL, Jia SR, Huang Y, Gao C, Wan YZ. *Mater. Lett* 2006;60:1710–1713.
13. Jongpaiboonkit L, Franklin-Ford T, Murphy WL. *Adv. Mater* 2009;21
14. Gao Y, Koumoto K. *Cryst. Growth Des* 2005;5:1983–2017.
15. Leveque I, Cusack M, Davis SA, Mann S. *Angew. Chem.-Int. Edit* 2004;43:885–888.
16. Green DW, Mann S, Oreffo ROC. *Soft Matter* 2006;2:732–737.
17. Kokubo T, Ito S, Huang ZT, Hayashi T, Sakka S, Kitsugi T, Yamamuro T. *J. Biomed. Mater. Res* 1990;24:331–343. [PubMed: 2156869]
18. Oyane A, Kim HM, Furuya T, Kokubo T, Miyazaki T, Nakamura T. *J. Biomed. Mater. Res., Part A* 2003;65A:188–195.
19. Miyaji F, Kim HM, Handa S, Kokubo T, Nakamura T. *Biomaterials* 1999;20:913–919. [PubMed: 10353645]
20. Yokogawa Y, Paz Reyes J, Mucalo MR, Toriyama M, Kawamoto Y, Suzuki T, Nishizawa K, Nagata F, Kamayama T. *J. Mater. Sci.: Mater. Med* 1997;8:407–412. [PubMed: 15348722]
21. Li PJ, Ohtsuki C, Kokubo T, Nakanishi K, Soga N, Nakamuro T. *J. Am. Ceram. Soc* 1992;75:2094–2097.

22. Barrere F, Snel MME, van Blitterswijk CA, de Groot K. *Biomaterials* 2004;25:2901–2910. [PubMed: 14962569]
23. Uchida M, Kim HM, Kokubo T, Miyaji F, Nakamura T. *J. Am. Ceram. Soc* 2001;84:2041–2044.
24. Murphy WL, Mooney DJ. *J. Am. Chem. Soc* 2002;124:1910–1917. [PubMed: 11866603]
25. Murphy WL, Kohn DH, Mooney DJ. *J. Biomed. Mater. Res* 2000;50:50–58. [PubMed: 10644963]
26. Zhang RY, Ma PX. *Macromol. Biosci* 2004;4:100–111. [PubMed: 15468200]
27. Bajpai AK, Singh R. *Polym. Int* 2007;56:557–568.
28. Tanahashi M, Yao T, Kokubo T, Minoda M, Miyamoto T, Nakamura T, Yamamuro T. *J. Am. Ceram. Soc* 1994;77:2805–2808.
29. Azevedo H, Leonor I, Alves C, Reis R. *Mater. Sci. Eng., C* 2005;25:169–179.
30. Liu Y, Hunziker EB, Randall NX, de Groot K, Layrolle P. *Biomaterials* 2003;24:65–70. [PubMed: 12417179]
31. Luong LN, Hong SI, Patel RJ, Outslay ME, Kohn DH. *Biomaterials* 2006;27:1175–1186. [PubMed: 16137760]
32. Yu X, Qu H, Knecht DA, Wei M. *J. Mater. Sci.: Mater. Med* 2009;20:287–294. [PubMed: 18763021]
33. Zhang R, Xu D, Landeryou T, Toth C, Dimaano N, Berry J, Evans J, Hawkins M. *J. Biomed. Mater. Res. A* 2004;71:412–418. [PubMed: 15472924]
34. Jayasuriya AC, Shah C. *J. Tissue Eng. Regen. Med* 2008;2:43–49. [PubMed: 18361482]
35. Leonor I, Azevedo H, Reis R. *Mater. Sci. Eng., C*. 2008 In Press.
36. Liu Y, de Groot K, Hunziker EB. *Ann. Biomed. Eng* 2004;32:398–406. [PubMed: 15095814]
37. Sogo Y, Ito A, Onoguchi M, Oyane A, Tsurushima H, Ichinose N. *Biomed. Mater* 2007;2:S175–S180. [PubMed: 18458464]
38. Stureson C, Carlfors J. *J. Controlled Release* 2000;67:171–178.
39. Berchane NS, Jebrail FF, Carson KH, Rice-Ficht AC, Andrews MJ. *J. Microencapsulation* 2006;23:539–552.
40. Heinonen JK, Lahti RJ. *Anal. Biochem* 1981;113:313–317. [PubMed: 6116463]
41. Eniola AO, Rodgers SD, Hammer DA. *Biomaterials* 2002;23:2167–2177. [PubMed: 11962658]
42. Fischer S, Forerg C, Ellenberger S, Merkle HP, Gander B. *J. Controlled Release* 2006;111:135–144.
43. Chesko J, Kazzaz J, Ugozzoli M, O'Haga DT, Singh M. *J. Pharm. Sci* 2005;94:2510–2519. [PubMed: 16200615]
44. Mu L, Feng SS. *J. Controlled Release* 2001;76:239.
45. Coombes AGA, Tasker S, Lindblad M, Holmgren J, Hoste K, Toncheva V, Schacht E, Davies MC, Illum L, Davis SS. *Biomaterials* 1997;18:1153–1161. [PubMed: 9259512]
46. Jabbarzadeh E, Nair LS, Khan YM, Deng M, Laurencin CT. *J. Biomater. Sci., Polym. Ed* 2007;18:1141–1152. [PubMed: 17931504]
47. Elliott, JC. *Structure and chemistry of the apatites and other calcium orthophosphates*. New York, NY: Elsevier; 1994.
48. He G, Dahl T, Veis A, George A. *Nat. Mater* 2003;2:552–558. [PubMed: 12872163]
49. Su X, Sun K, Cui FZ, Landis WJ. *Bone* 2003;32:150–162. [PubMed: 12633787]
50. Fazan F, Marquis PM. *J. Mater. Sci.: Mater. Med* 2000;11:787–792. [PubMed: 15348061]
51. Lin JHC, Kuo KH, Ding SJ, Ju CP. *J. Mater. Sci.: Mater. Med* 2001;12:731–741. [PubMed: 15348246]
52. Driessens FCM, van Dijk JWE, Borggreven JPM. *Calcif. Tissue Res* 1978;26:127–137. [PubMed: 32960]
53. Ruhe PQ, Boerman OC, Russel FGM, Spauwen PHM, Mikos AG, Jansen JA. *J. Controlled Release* 2005;106:162–171.
54. Matsumoto T, Okazaki M, Inoue M, Yamaguchi S, Kusunose T, Toyonaga T, Hamada Y, Takahashi J. *Biomaterials* 2004;25:3807–3812. [PubMed: 15020156]
55. He G, Gajjeraman S, Schultz D, Cookson D, Qin CL, Butler WT, Hao JJ, George A. *Biochemistry* 2005;44:16140–16148. [PubMed: 16331974]
56. Raman C, Berklund C, Kim K, Pack DW. *J. Controlled Release* 2005;103:149–158.
57. LeGeros RZ. *Clin. Orthop. Relat. Res* 2002;395:81–98. [PubMed: 11937868]

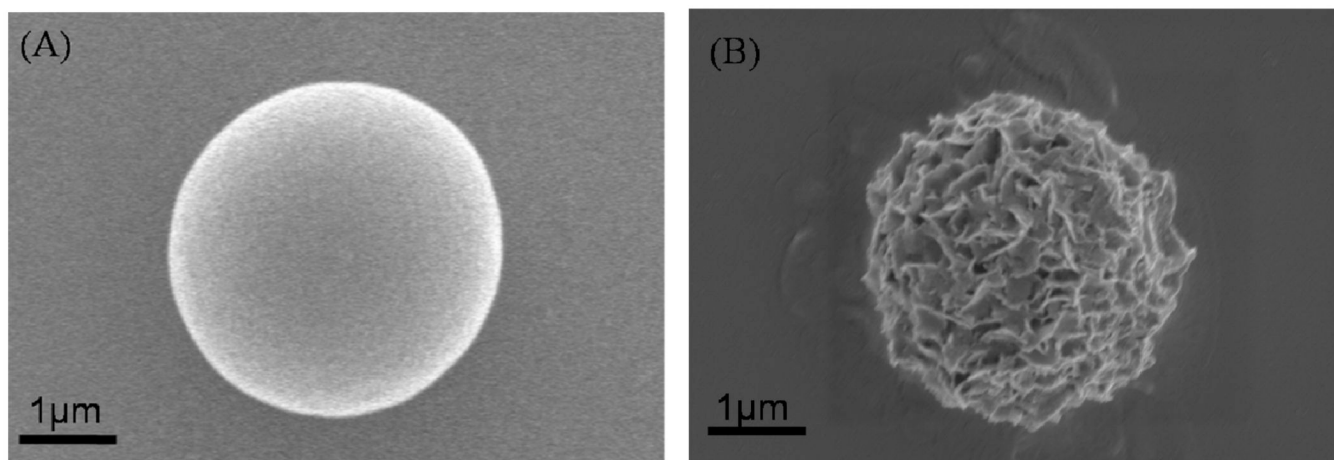


Figure 1. PLG microsphere (A) and mineral-coated microsphere after incubation in mSBF for 7 days (B).

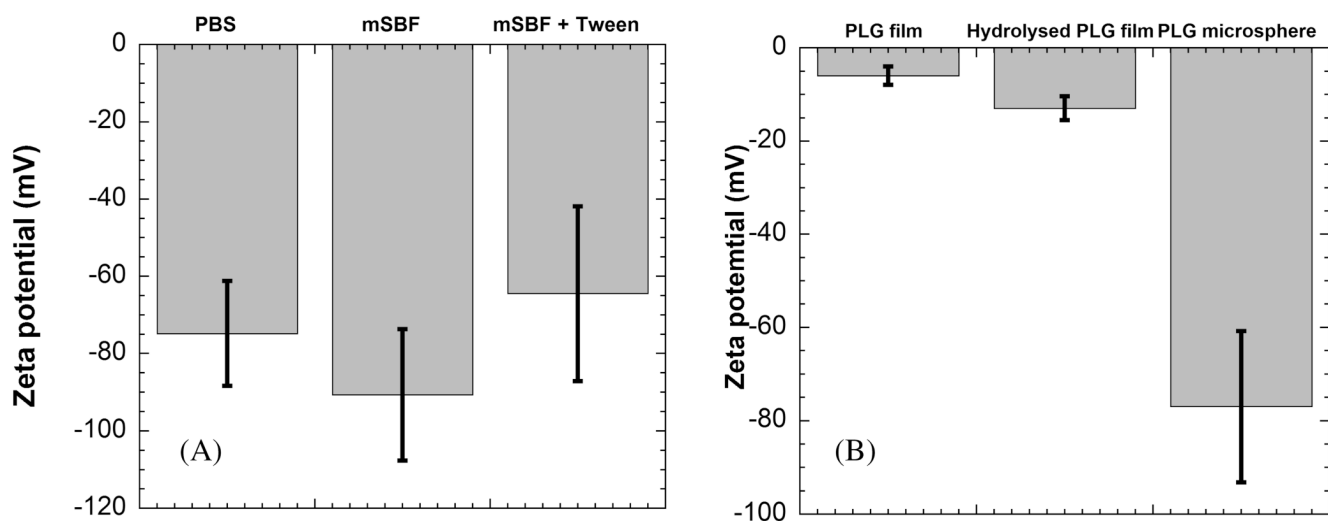


Figure 2. Zeta potential of (A) PLG microspheres in buffers PBS, mSBF, and mSBF + 0.1% v/v Tween20™, and (B) non-hydrolysed and hydrolysed PLG films in comparison with PLG microspheres.

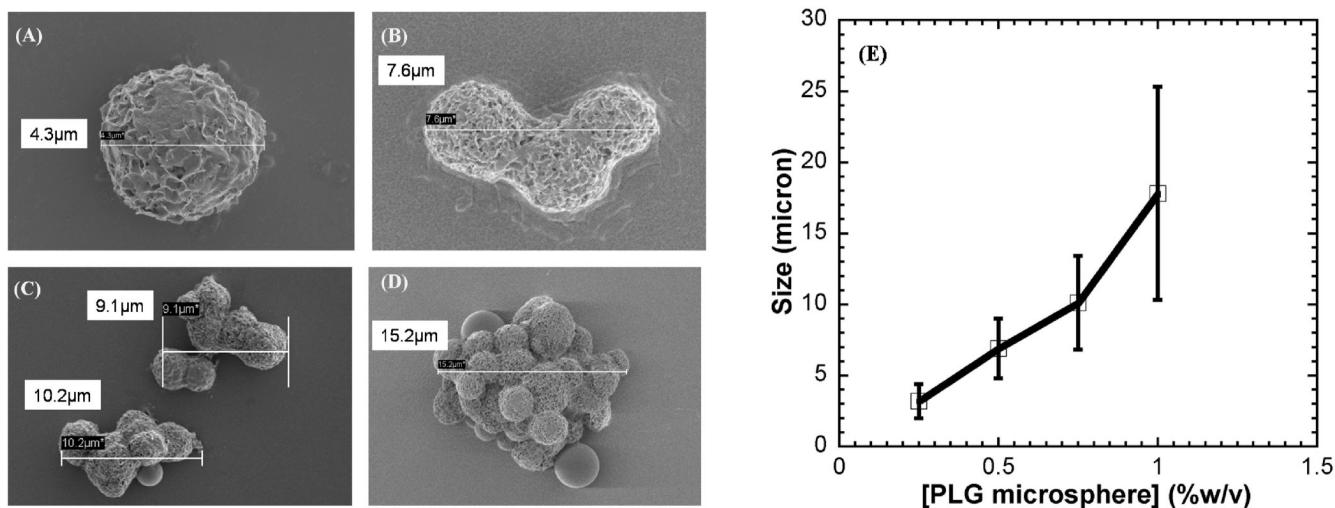


Figure 3. SEM images of mineral-coated microspheres after a 7 day incubation in mSBF solution, (A) 0.25% w/v, (B) 0.50% w/v, (C) 0.75% w/v, and (D) 1.00% w/v. (E) Relationship between the microsphere concentration in solution during mineral growth, and the size of mineral-coated microsphere aggregates.

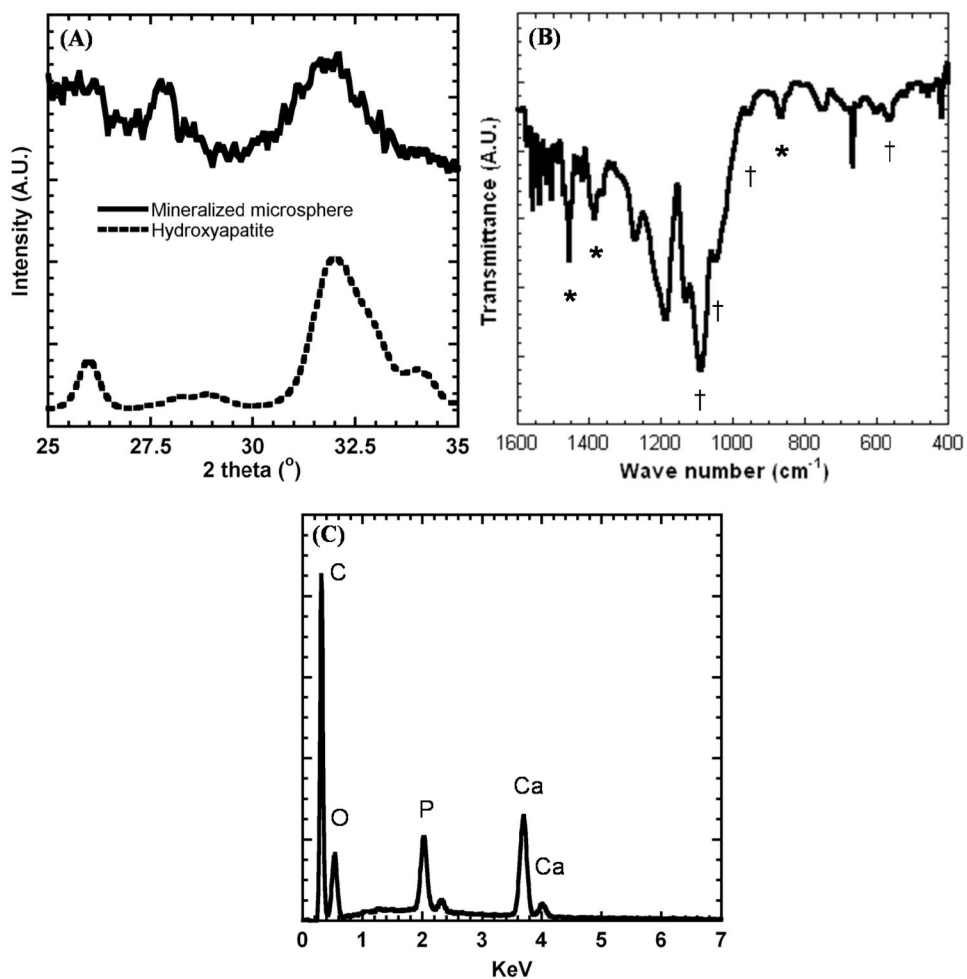


Figure 4. (A) X-ray diffraction analysis of mineral-coated microspheres and hydroxyapatite powder (included for comparison), (B) Fourier transform infrared analysis of mineral-coated microspheres. Peaks associated with carbonate are denoted by *, and peaks associated with phosphate are denoted by †. (C) EDS spectrum of mineral-coated microspheres after a 7 day incubation in mSBF.

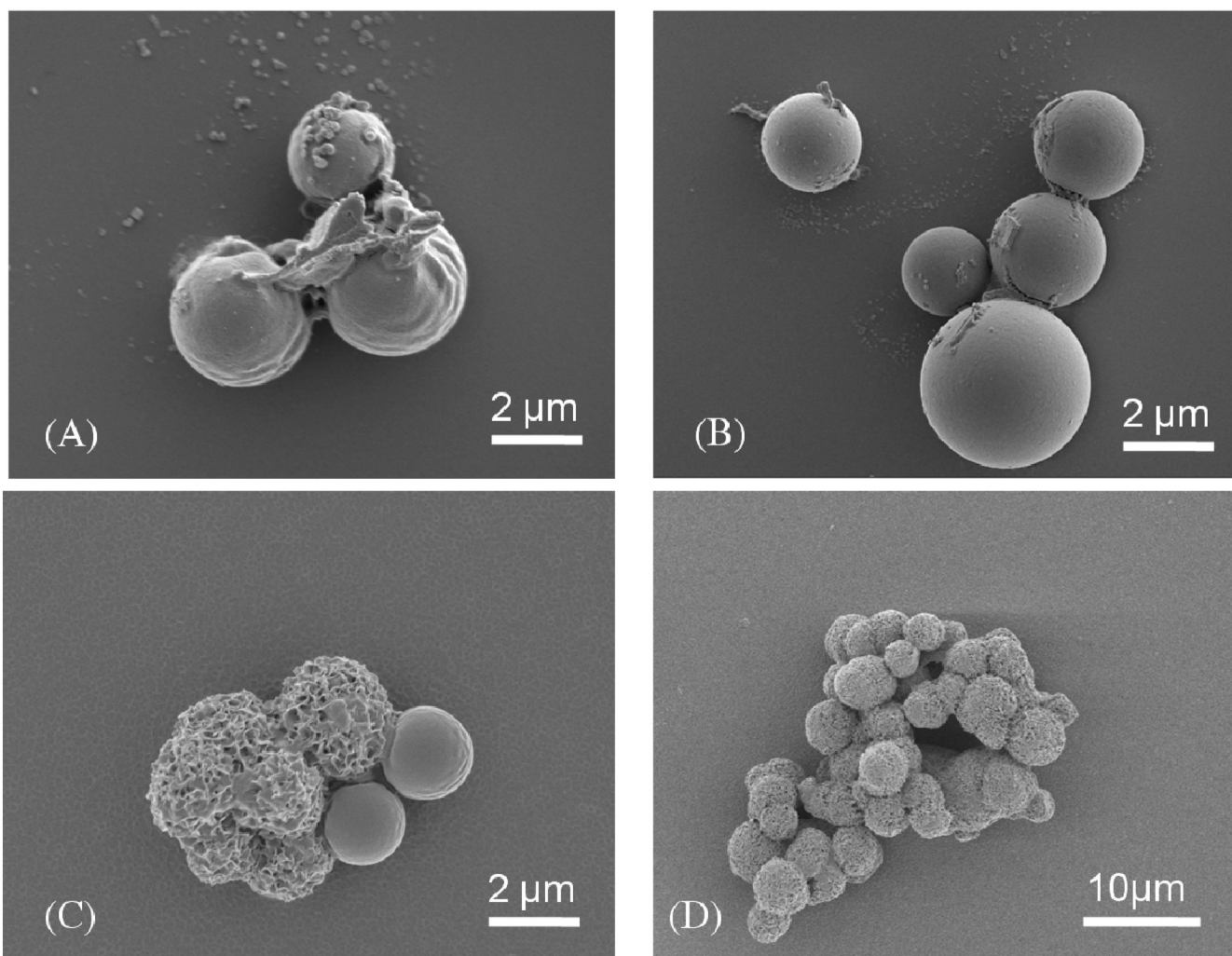


Figure 5. The process of mineral nucleation and growth on PLG microspheres. SEM images of microspheres after: (A) the first day of immersion in mSBF, (B) day 3 of incubation, (C) day 5 of incubation, (D) day 7 of incubation.

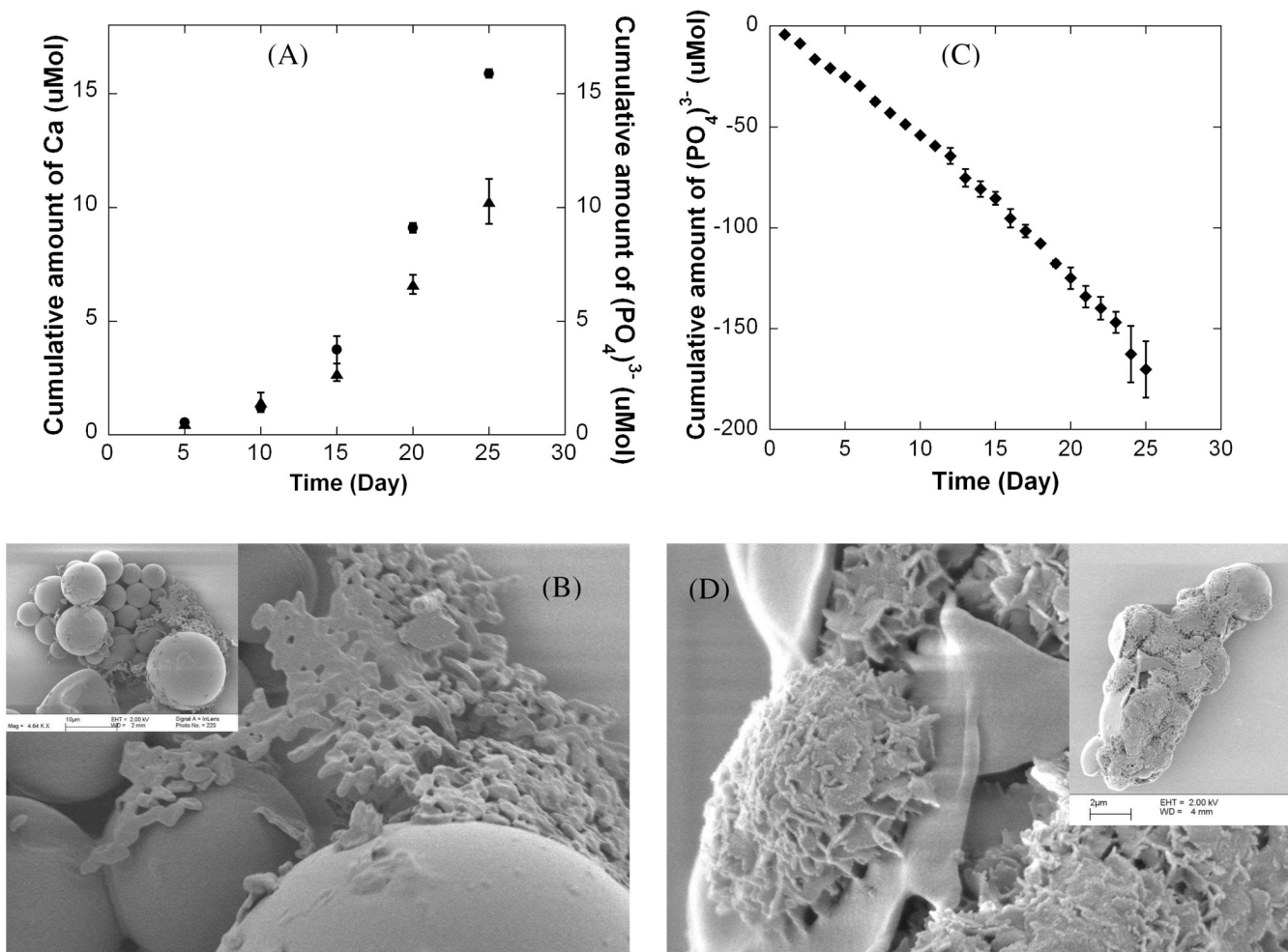


Figure 6. (A) Cumulative dissolution of Ca²⁺ and PO₄³⁻ during a 25 day incubation in tris-buffered saline (TBS), and (B) SEM images of mineral-coated microspheres after the 25 day TBS incubation. (C) Cumulative dissolution of PO₄³⁻ during a 25 day incubation in DMEM, and (D) SEM images of mineral-coated microspheres after the 25 day DMEM incubation.

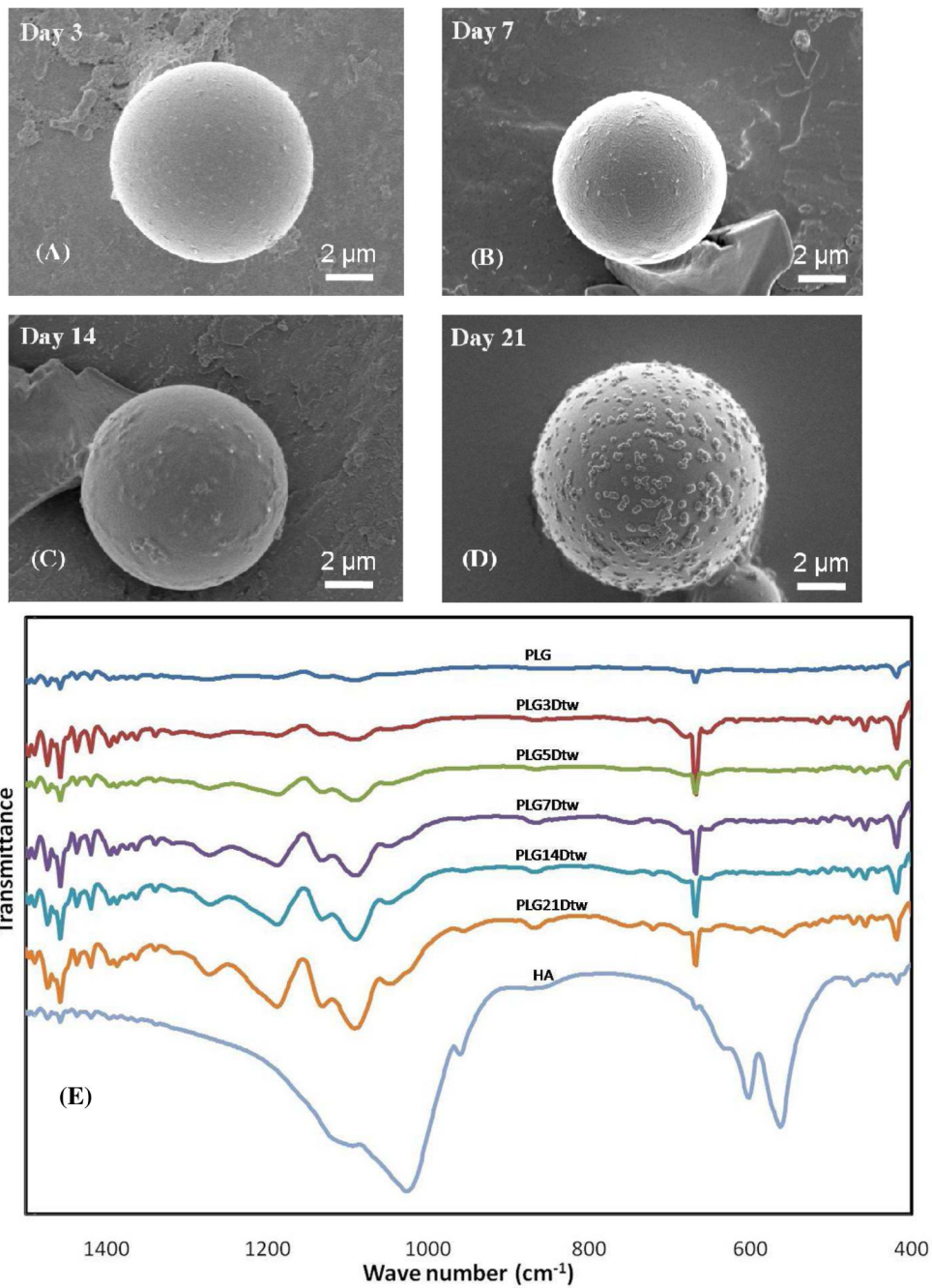


Figure 7. Effect of surfactant (Tween 20TM) on the mineral formed on the PLG microsphere surfaces (A) after 3 days, (B) after 7 days, (C) after 14 days, and (D) after 21 days. (E) FTIR spectrum of PLG microspheres coated with mineral via a 21 days mSBF incubation in the presence of 0.1% v/v Tween20TM. A spectrum of commercial HA powder is included for comparison.

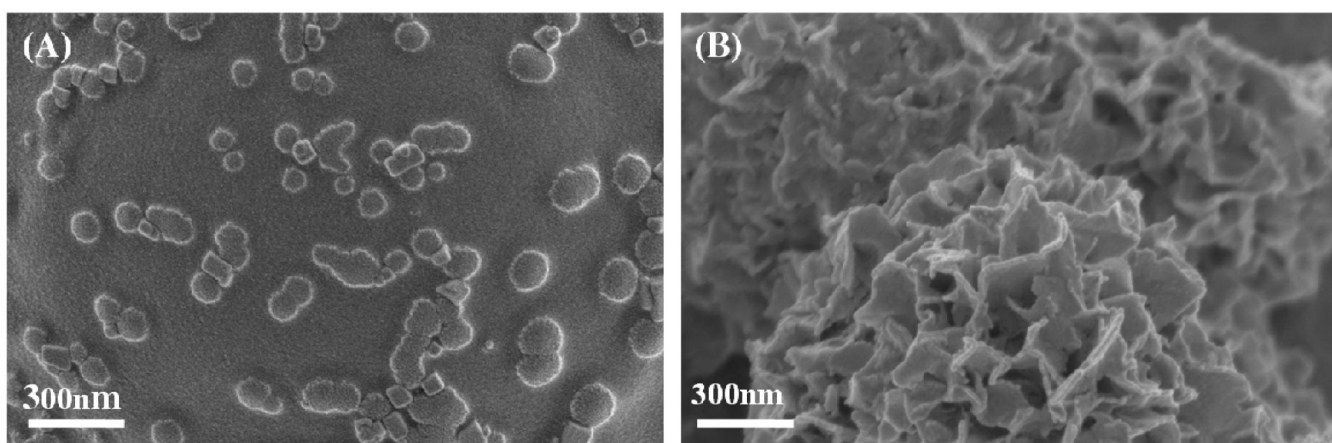


Figure 8. Nanometer-scale mineral morphology on the surface of microspheres formed (A) in the presence of 0.1% v/v Tween20™, and (B) in the absence of Tween20™.